Journal of
Radiation Protection and Research 2016;41(4):344-349
https://doi.org/10.14407/jrpr.2016.41.4.344

pISSN 2508-1888 | eISSN 2466-2461

# Measurement of Neutron Production Double-differential Cross-sections on Carbon Bombarded with 430 MeV/Nucleon Carbon Ions

**Yutaro Itashiki[1,*], Youichi Imahayashi[1], Nobuhiro Shigyo[1], Yusuke Uozumi[1], Daiki Satoh[2], Tsuyoshi Kajimoto[3], Toshiya Sanami[4], Yusuke Koba[5], Naruhiro Matsufuji[5]**

*[1]Department of Applied Quantum Physics and Nuclear Engineering, Kyushu University, Fukuoka, Japan; [2]Nuclear Science and Engineering Center, Japan Atomic Energy Agency, Ibaraki, Japan; [3]Division of Energy and Environmental Engineering, Hiroshima University, Hiroshima, Japan; [4]Radiation Science Center, High Energy Accelerator Research Organization, Ibaraki, Japan; [5]National Institute of Radiological Sciences, National Institutes for Quantum and Radiological Science and Technology, Chiba, Japan*

ABSTRACT

**Background:** Carbon ion therapy has achieved satisfactory results. However, patients have a risk to get a secondary cancer. In order to estimate the risk, it is essential to understand particle transportation and nuclear reactions in the patient's body. The particle transport Monte Carlo simulation code is a useful tool to understand them. Since the code validation for heavy ion incident reactions is not enough, the experimental data of the elementary reaction processes are needed.

**Materials and Methods:** We measured neutron production double-differential cross-sections (DDXs) on a carbon bombarded with 430 MeV/nucleon carbon beam at PH2 beam line of HIMAC facility in NIRS. Neutrons produced in the target were measured with NE213 liquid organic scintillators located at six angles of 15, 30, 45, 60, 75, and 90°.

**Results and Discussion:** Neutron production double-differential cross-sections for carbon bombarded with 430 MeV/nucleon carbon ions were measured by the time-of-flight method with NE213 liquid organic scintillators at six angles of 15, 30, 45, 60, 75, and 90°. The cross sections were obtained from 1 MeV to several hundred MeV. The experimental data were compared with calculated results obtained by Monte Carlo simulation codes PHITS, Geant4, and FLUKA.

**Conclusion:** PHITS was able to reproduce neutron production for elementary processes of carbon-carbon reaction precisely the best of three codes.

**Keywords:** Carbon ion therapy, Neutron DDX, PHITS, Geant4, FLUKA

Original Research

**Received** July 17, 2015
**Revision** September 26, 2016
**Accepted** October 24, 2016

**Corresponding author:** Yutaro Itashiki

744 Motooka, Nishi-ku, Fukuoka 819-0395, Japan
Tel: +81-92-802-3484,
Fax: +81-92-802-3484,
E-mail: k0uc.ik8imai@gmail.com



## Introduction

Carbon ion therapy has achieved satisfactory results because of the advantages of high curability and minimally invasiveness. In National Institute of Radiological Sciences (NIRS), the number of patients receiving carbon ion therapy from June 1994 to March 2014 was 8227.[1)] However, patients have a risk to get a secondary cancer. As a specific example, there was a report that lifetime cancer risk due to secondary neutrons in the proton therapy was 5-10% [1]. In order to estimate the risk precisely, it is essential to un-

[1)] http://www.nirs.go.jp/hospital/result/pdf/2014_03.pdf.

derstand particle transportation and nuclear reactions in a patient's body. The particle transport Monte Carlo simulation code is a useful tool to understand them. Since the code validation for heavy ion incident reactions is not enough, the experimental data of the elementary reaction processes as neutron production cross section are needed.

We previously measured neutron production double-differential cross-sections (DDXs) on a carbon bombarded with 290 MeV/nucleon carbon ions and confirmed that the Monte-Carlo simulation code PHITS [2] reproduced the experimental data [3]. In this article, we report the neutron production DDXs on a carbon bombarded with 430 MeV/nucleon carbon ions which is the maximum energy beam used in the therapy. Then, the experimental DDXs were compared with calculated DDXs by Monte Carlo simulation codes as PHITS, Geant4 [4], and FLUKA [5].

## Materials and Methods

### 1. Experiment

The experiment was performed at PH2 beam line of HIMAC facility in NIRS. The experimental set-up is shown on Figure 1.

The 430 MeV/nucleon carbon beam was irradiated on a 5 cm × 5 cm × 1 cm graphite target rotated 45° to the beam axis in order to reduce multiple scattering neutrons emitted in the direction of 90°.

A 0.5 mm thick NE102A plastic scintillator (Beam pick up detector) was placed in front of the target to monitor beam intensity. The beam intensity was set to around $10^5$ particles per spill to reduce the beam signal pile-up. Neutrons produced in the target were measured with two sizes of NE213 liquid organic scintillators located at six angles of 15, 30, 45, 60, 75, and 90°. The 5.08 cm long one (Small neutron detector) was used to obtain the neutron spectra from 1 MeV to 10 MeV and the 12.7 cm long one (Large neutron detector) was used above 5 MeV. To determine signal bias level, light outputs of the neutron detectors were calibrated with γ-ray sources as $^{241}$Am, $^{133}$Ba, $^{137}$Cs, $^{60}$Co, and $^{241}$Am-Be. The 2 mm thick NE102A scintillators (Veto detector) to discriminate charged particles were set in front of the neutron detectors.

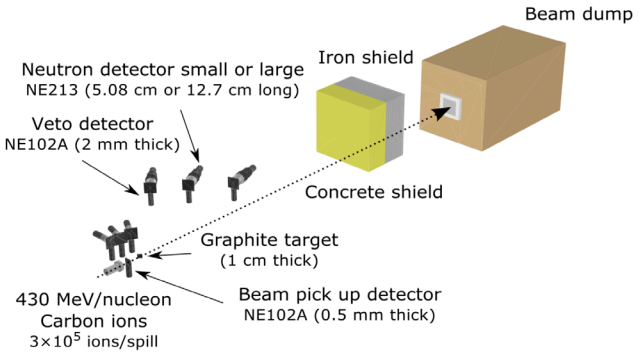


Fig. 1. The experimental set-up at PH2 beam line of HIMAC facility in NIRS.

Kinetic energies of neutrons were determined by the time-of-flight (TOF) method. The flight path lengths from the target were set to 1.0-2.5 m for neutron small detectors and 1.6-3.9 m for neutron large detectors.

Background neutrons were estimated by a measurement with iron shadow bars between the target and the neutron detectors (measurement B). Neutrons emitted from the target to the neutron detectors directly were obtained by subtracting neutrons for the measurement B from neutrons for a measurement without iron shadow bars (measurement A).

An electronic circuit for data acquisition consisted of NIM and CAMAC modules. The light output of the neutron detector was registered with analog-to-digital converter (ADC) and the time difference between the signal of the neutron detector and the signal of the beam pick up detector was registered with time-to-digital converter (TDC).

### 2. Analysis

1) Determination of neutron kinetic energy

Figure 2 shows the inverse TOF spectrum for the large neutron detector at 15°. TDC of the horizontal axis is the time difference between the start signal of the neutron detector and the stop signal of the beam pick up detector. The peak

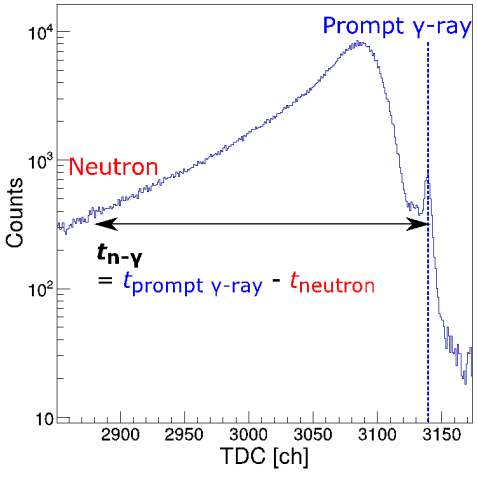


Fig. 2. Inverse TOF spectrum for the large neutron detector at 15°.

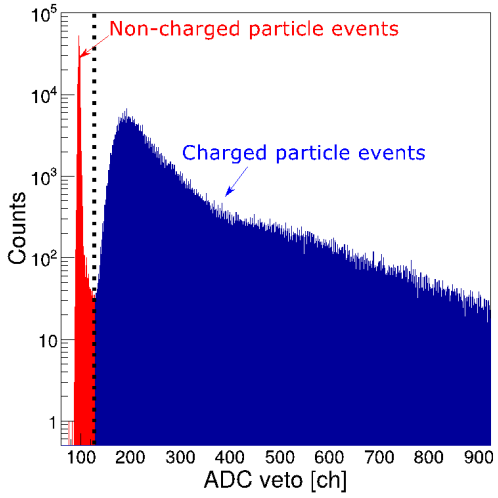


Fig. 3. Light output spectrum for the veto detector.

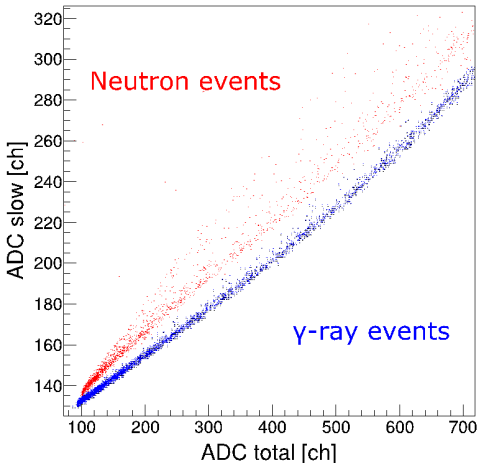


Fig. 4. Two-dimensional histogram of the light output for the neutron detector.

corresponding to the prompt γ-ray events appears at 3140 ch. The neutron kinetic energy $E_n$ was determined by using the following formula:

$$E_n = \frac{m_n c^2}{\sqrt{1-\left(\frac{L}{ct_{n-\gamma}+L}\right)^2}} - m_n c^2 \quad (1)$$

where $m_n$ is the rest mass of neutron, $L$ is distance from the target to the neutron detector, $c$ is velocity of light and $t_{n\text{-}\gamma}$ is difference of flight time between the prompt γ-ray peak and the neutron.

2) Extraction of neutron events

In Figure 2, not only neutron events but also γ-ray and charged particle ones are included.

Non-charged particle events as neutrons and γ-rays were extracted by using the light output spectrum of the veto detector in Figure 3. The detector signals come from energy deposition of charged particles via the Coulomb interaction. Non-charged particles do not deposit their energy in the veto detector because the detector is so thin that they are not able to cause nuclear reactions. Therefore, non-charged particle events were registered as offset values. The events below 125 channels were extracted as non-charged particle events.

Neutron events were extracted by using the two-gate integration method [6]. In Figure 4, the horizontal axis of the histogram as ADC total is the integrated value of the signal for the neutron detector and the vertical axis of the histogram as ADC slow is the integrated value of the delayed part of the signal for the neutron detector. In the neutron detector, the rate of the delayed part of the signal for neutron is larger than that for γ-ray. The events painted red in Figure 4 were extracted as neutron events.

3) Estimation of neutron detection efficiency

Neutron detection efficiency of the neutron detector was estimated by using SCINFUL-QMD code [7, 8]. This code can calculate light output response function of a liquid organic scintillator for neutron energies up to 3 GeV and detection efficiency is obtained by integrating the response function above a bias level. For neutron below 150 MeV, 11 initial reaction channels are prepared. For neutron above 150 MeV, proton, and pion, the quantum molecular dynamics incorporated with the statistical decay model (QMD+SDM) is used. The bias level for determining the detection efficiency was a light output (MeVee) corresponding to a minimum ADC total channel of the neutron events in Figure 4. In this analysis, the bias level for the small neutron detector was set to 0.073 MeVee and that for the large neutron detector was set to 1.041 MeVee. Figure 5 shows the neutron detection efficiencies for small and large neutron detectors.

4) Derivation of neutron production DDX

Neutron production DDX was derived from the following formula:

$$\frac{d^2\sigma}{dE\,d\Omega}(E) = \frac{N_n(E)\,f}{N_{ion}\,\rho\,\varepsilon(E)\,\Delta E\,\Delta\Omega} \quad (2)$$

where $N_n(E)$ is the number of detected neutrons, $N_{ion}$ is the number of carbon beam, $\rho$ is the surface density of the target, $\varepsilon(E)$ is the neutron detection efficiency, $\Delta E$ is the energy bin


https://doi.org/10.14407/jrpr.2016.41.4.344

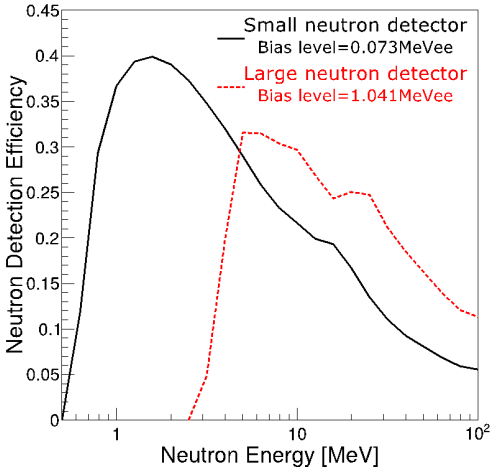


Fig. 5. Neutron detection efficiencies for small and large neutron detectors calculated by SCINFUL-QMD code.

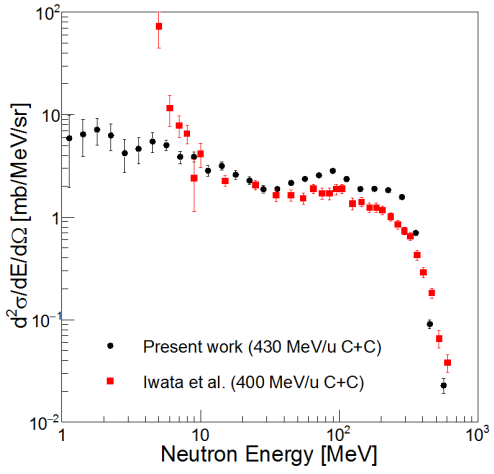


Fig. 6. Neutron production DDXs at 30°.

width, $\Delta\Omega$ is the solid angle for each neutron detector, and $f$ is a factor which corrects data acquisition and $N_{ion}$.

In this analysis, experimental DDX ($DDX_{exp}$) was obtained by subtracting results for the measurement B from results for the measurement A. $DDX_{exp}$ obtained by the small neutron detector was adopted below 5 MeV and $DDX_{exp}$ obtained by the large neutron detector was adopted above 5 MeV.

In this experiment, the carbon target was 1 cm thick and much thicker than ideal target for DDX measurement. In this analysis, an effect of multiple scattering in the target was estimated by using the simulation code PHITS. DDX was obtained by multiplying the $DDX_{exp}$ by the ratio of DDX calculated with $0.01 \times 0.01 \times 0.01$ cm target to DDX calculated with $5 \times 5 \times 1$ cm target rotated 45° to the beam axis.

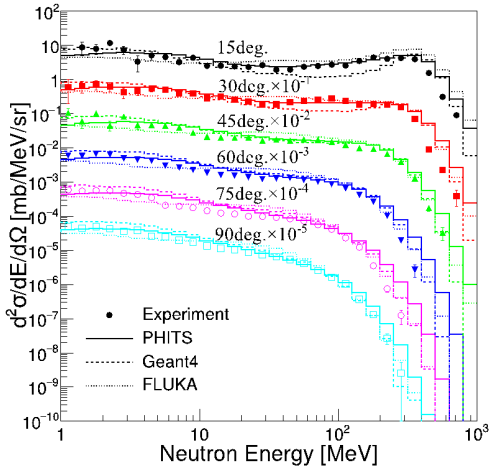


Fig. 7. Neutron production DDXs at 15, 30, 45, 60, 75, and 90°after the multiple scattering correction.

### 3. Simulation

Neutron production DDX was calculated with Monte Carlo simulation codes PHITS, Geant4, and FLUKA to estimate the accuracy of these codes. The versions of these codes are PHITS 2.81, Geant4 10.1, and FLUKA 2011.2c.0 respectively. A $0.01 \times 0.01 \times 0.01$ cm carbon target was irradiated with 430 MeV/nucleon carbon beam. To shorten calculation time, ring neutron detectors were adopted [3]. For Nucleus-Nucleus collision models, PHITS, Geant4, and FLUKA adopt JQMD, G4QMD, and RQMD, respectively. For total cross sections for Nucleus-Nucleus collision, we used KUROTAMA model [9], Glauber model with Gribov corrections [10], and default model for PHITS, Geant4, and FLUKA, respectively.

## Results and Discussion

Figure 6 shows the experimental results at 30° compared with the data of 400 MeV/nucleon carbon ions incident on carbon measured by Iwata et al. [11]. They show an agreement within a factor of 1.3 in the energy region above 10 MeV.

Figure 7 shows neutron production DDXs for carbon bombarded with 430 MeV/nucleon carbon ions obtained at six angles of 15, 30, 45, 60, 75, and 90° after the multiple scattering correction. Furthermore, DDXs calculated with PHITS, Geant4, and FLUKA are shown with the experimental data. The experimental data below 3 MeV for 15° and 45° were not smooth because the ratio of background neutrons to foreground neutrons was large. These codes reproduce the experimental data in the whole energy.

Figure 8 shows neutron angular distributions obtained by

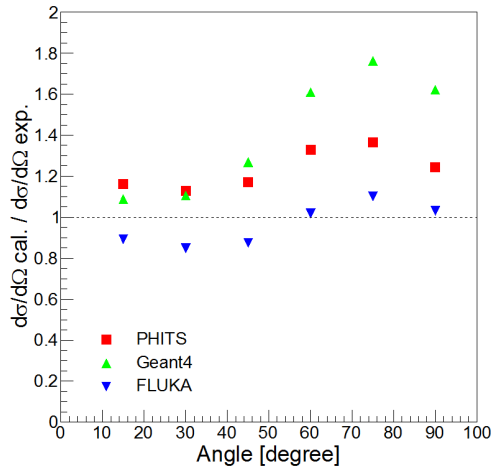


Fig. 8. Neutron angular distributions from 1 MeV to 20 MeV calculated with PHITS, Geant4, and FLUKA, normalized by experimental data.

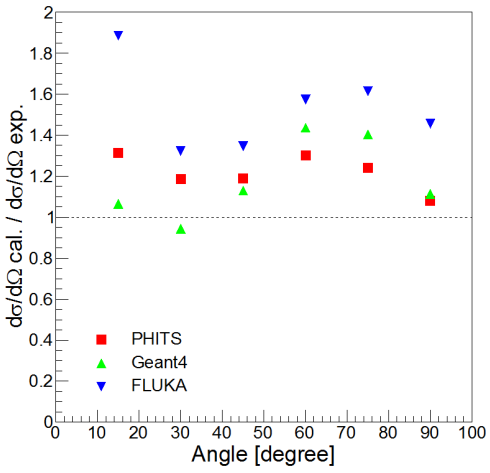


Fig. 9. Neutron angular distributions from 20 MeV to 1 GeV calculated with PHITS, Geant4, and FLUKA normalized by experimental data.

integrating calculated DDXs from 1 MeV to 20 MeV normalized by the experimental data. Neutrons from 1 MeV to 20 MeV are produced by both QMD and evaporation process. Both PHITS and FLUKA reproduce shape of angular distributions and absolute values well. Geant4 overestimates the experimental data as an angle against the beam axis becomes larger.

Figure 9 shows neutron angular distributions obtained by integrating calculated DDXs from 20 MeV to 1 GeV normalized by the experimental data. The majority of neutrons from 20 MeV to 1 GeV are produced by QMD process. PHITS reproduces shape of angular distributions and absolute values well. FLUKA does not reproduce shape of angular distributions and overestimates absolute values. In particular, FLUKA overestimates experimental result 1.9 times at 15°. Geant4 does not reproduce shape of angular distributions.

## Conclusion

Neutron production DDXs for carbon bombarded with 430 MeV/nucleon carbon ions were measured at PH2 beam line of HIMAC facility in NIRS. We obtained the DDXs above 1MeV at six angles of 15, 30, 45, 60, 75, and 90°. The DDXs were compared with DDXs calculated with Monte Carlo simulation codes as PHITS, Geant4, and FLUKA. PHITS reproduced the experimental DDXs the best of three codes.

We confirmed PHITS code was able to reproduce neutron production for elementary processes of carbon-carbon reaction precisely. We hope estimation of lifetime cancer risk due to secondary neutrons in the carbon therapy by using Monte Carlo simulation codes will come true.

## References

1. Brenner DJ, Hall EJ. Secondary neutrons in clinical proton radiotherapy: A charged issue. Radiother. Oncol. 2008;86:165-170.
2. Sato T, et al. Particle and heavy ion transport code system PHITS, Version 2.52. J. Nucl. Sci. Technol. 2013;50:9:913-923.
3. Satoh D, et al. Measurement of neutron-production double-differential cross-sections on carbon bombarded with 290-MeV/nucleon carbon and oxygen ions. Nucl. Instrum. Methods A. 2011;644:59-67.
4. Agostinelli S, et al. Geant4, A Simulation Toolkit. Nucl. Instrum. Methods A. 2003; 506:250-303.
5. Bohlen TT, et al. The FLUKA code: Developments and challenges for high energy and medical applications. Nucl. Data Sheets. 2014;120:211-214.
6. Zucker MS, Tsoupas N. An n-γ pulse discrimination system for wide energy ranges. Nucl. Instrum. Methods A.1990;299:281-285.
7. Satoh D, Sato T, Shigyo N, Ishibashi K. SCINFUL-QMD: Monte Carlo based computer code to calculate response function and detection efficiency of a liquid organic scintillator for neutron energies up to 3 GeV. JAEA-Data/Code 2006;2006-023:1-20.
8. Satoh D, Sato T, Endo A, Yamaguchi Y, Takada M, Ishibashi K. Measurement of response functions of liquid organic scintillator for neutrons up to 800 MeV. J. Nucl. Sci. Technol. 2006;43:714-719.
9. Iida K, Kohama A, Oyamatsu K. Formula for proton-nucleus reaction cross section at intermediate energies and its application.

 https://doi.org/10.14407/jrpr.2016.41.4.344

J. Phys. Soc. Japan. 2007;76:044201.
10. Franco V. High-energy nucleus-nucleus collisions. I. general theory and applications to deuteron-deuteron scattering. Phys. Rev. 1968;175:1376-1393.
11. Iwata Y, et al. Double-differential cross-sections for the neutron production from heavy-ion reactions at energies E/A=290-600 MeV. Phys. Rev. C. 2001;64:054609.